Simultaneous Micropatterning of Fibrous Meshes and Bioinks for the Fabrication of Living Tissue Constructs

Mylène de Ruijter, Alexandre Ribeiro, Inge Dokter, Miguel Castilho,* and Jos Malda*

Fabrication of biomimetic tissues holds much promise for the regeneration of cells or organs that are lost or damaged due to injury or disease. To enable the generation of complex, multicellular tissues on demand, the ability to design and incorporate different materials and cell types needs to be improved. Two techniques are combined: extrusion-based bioprinting, which enables printing of cell-encapsulated hydrogels; and melt electrowriting (MEW), which enables fabrication of aligned (sub)-micrometer fibers into a single-step biofabrication process. Composite structures generated by infusion of MEW fiber structures with hydrogels have resulted in mechanically and biologically competent constructs; however, their preparation involves a two-step fabrication procedure that limits freedom of design of microfiber architectures and the use of multiple materials and cell types. How convergence of MEW and extrusion-based bioprinting allows fabrication of mechanically stable constructs with the spatial distributions of different cell types without compromising cell viability and chondrogenic differentiation of mesenchymal stromal cells is demonstrated for the first time. Moreover, this converged printing approach improves freedom of design of the MEW fibers, enabling 3D fiber deposition. This is an important step toward biofabrication of voluminous and complex hierarchical structures that can better resemble the characteristics of functional biological tissues.

M. de Ruijter, A. Ribeiro, I. Dokter, Dr. M. Castilho, Prof. J. Malda
Department of Orthopedics
University Medical Center Utrecht
Utrecht University
P.O. Box 85500, 3508 GA Utrecht, The Netherlands
E-mail: m.diascastilho@umcutrecht.nl; j.malda@umcutrecht.nl
M. de Ruijter, A. Ribeiro, I. Dokter, Dr. M. Castilho, Prof. J. Malda
Regenerative Medicine Center Utrecht
Uppsalalaan 8, 3584 CT Utrecht, The Netherlands
Dr. M. Castilho
Department of Biomedical Engineering Eindhoven University
of Technology
P.O. Box 513, 5600 MB Eindhoven, The Netherlands
Prof. J. Malda
Department of Equine Sciences Faculty of Veterinary Sciences
Utrecht University
Yalelaan 112, 3584 CM Utrecht, The Netherlands

The ORCID identification number(s) for the author(s) of this article can be found under https://doi.org/10.1002/adhm.201800418.

Biofabrication is a rapidly advancing field that uses bioprinting or bioassembly to create organized 3D structures that are biologically functional.[1] These engineered biological constructs can be used for drug discovery and screening, for the development of in vitro models of human disease or ultimately, as implants to restore or replace damaged tissue.[2–4] In order to successfully engineer a biologically functional construct, it is essential to stimulate neo-tissue formation and improve spatial organization and mechanical integrity as seen in native tissues.[5–7] Extrusion-based bioprinting techniques are already used to generate hydrogel constructs that replicate some native tissue features, such as zonal organization of articular cartilage tissue, and can generate vascularized tissue structures, bone tissue gradients, and the air–blood barrier by using different materials, cell types, and cell densities.[8–12] However, hydrogels that support extensive cellular differentiation are intrinsically soft and thus mechanically unstable.[13] This challenge can potentially be resolved with fiber reinforcing strategies, including adaptation of textile techniques that enable fabrication of 3D-woven networks.[14–16] However, these techniques are limited in control over material or cell deposition. Fused deposition modeling (FDM) does allow for hydrogel reinforcement and control over cell deposition. Unfortunately, the relatively low printing resolution (≈200 μm) of the reinforcing material with FDM limits space for tissue maturation,[17–22] and this reinforcing strategy usually fails to provide an adequate micromechanical environment for tissue differentiation.[23] An alternative strategy to reinforce hydrogels involves the incorporation of sub-micron scale, organized fiber scaffolds generated by melt electrowriting (MEW).[24–28] This electrohydrodynamic fiber writing uses a high voltage electrical field to form sub-micrometer fibers from polymer melts. Previous studies show that MEW fibers used to fabricate 3D screening devices to test cellular response to microstructures fibers can facilitate the specific alignment of cells.[29,30] However, this fabrication procedure requires a two-step approach—the fabrication of the fiber scaffold, followed by embedding a cell-laden hydrogel inside—which severely limits control over accurate deposition of multimaterials and cells, and subsequently the creation of hierarchical structures.

The aim of this study was to generate biologically functional constructs with more complex architecture and composition by

**ADVANCED
SCIENCE NEWS**
www.advancedsciencenews.com

**ADVANCED
HEALTHCARE
MATERIALS**
www.advhealthmat.de

converging MEW and extrusion-based bioprinting into a single-step manufacturing procedure. Here, we demonstrate that this combination increases freedom of design, while maintaining the specific advantages associated with each of the individual techniques.

To illustrate generation of organized cellular structures, equine-derived mesenchymal stromal cells (eMSCs) were labeled with fluorescent dyes, embedded in 10% gelatin-metacryloyl (gelMA) and simultaneously printed with polycaprolactone (PCL) MEW fibers (**Figure 1**A). Precise arrangement of cells and materials in 3D was demonstrated by filling the pores of micro fiber scaffolds with extruded *Tetris*-like shapes of eMSC-laden gels (Figure 1B). Fine control over cell deposition was shown in both in-plane (*x*- and *y*-axis) printing (Figure 1C,D) and out-of-plane (*z*-axis) printing (Figure 1E). The 13 µm diameter of the MEW fibers (PCL), compared with the 200–400 µm diameter of the extruded bioink (gelMA), emphasizes the low volume of PCL in this multiscale fabrication process. The resolution of converged printing is currently limited by the resolution of hydrogel deposition. Nonetheless, the MEW boxes contribute to the shape fidelity of the printed hydrogel. Therefore, the 200–400 µm diameter of the extruded gelMA was relatively smaller compared with previously reported diameters of >500 µm.[11,31] Precise control over the deposition of the cell-containing bioink also provides the opportunity to control porosity and pore shape in the composite constructs
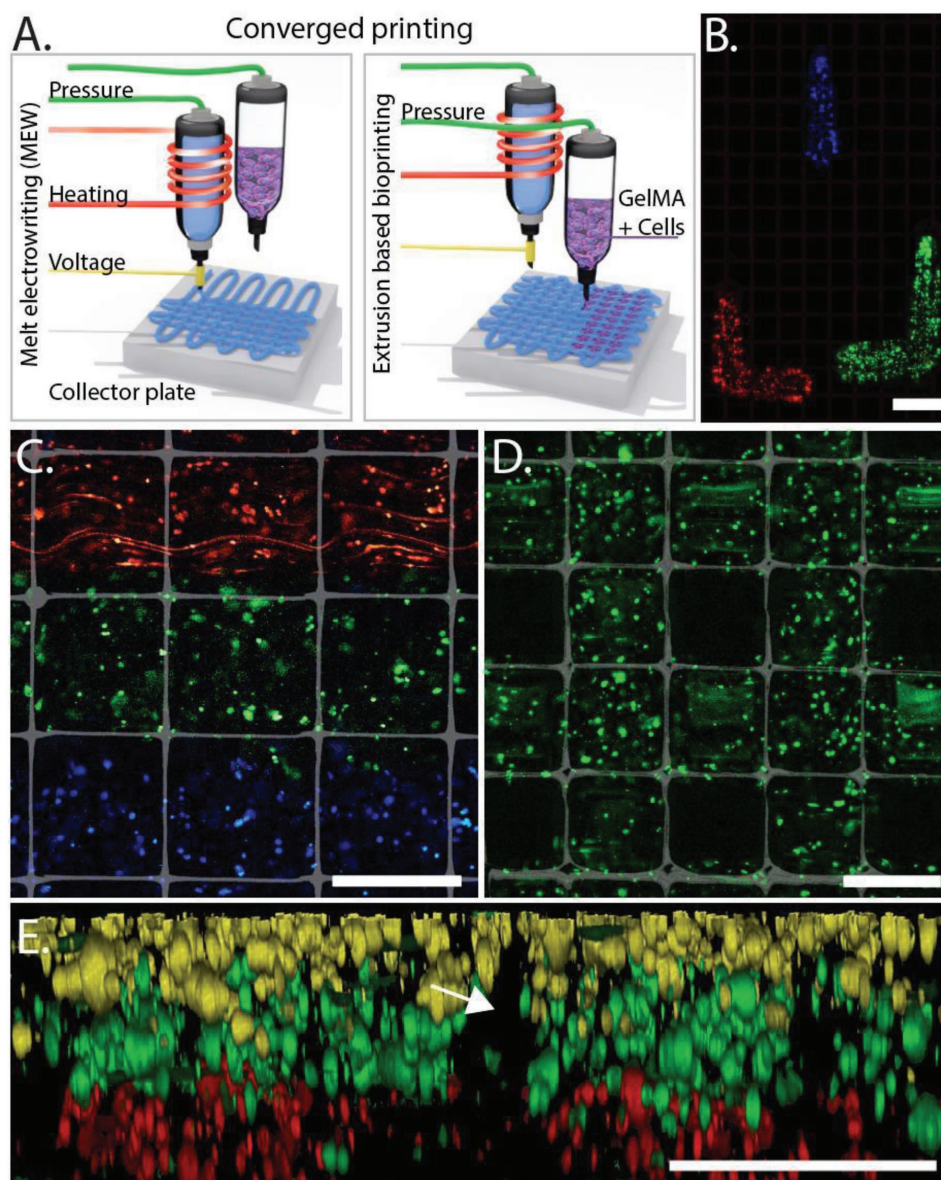
Figure 1. Convergence of MEW (PCL) and extrusion-based bioprinting (gelMA) into a single-step approach A) allows for control over spatial placement of cells. Control over positioning of cells (membrane-labeled eMSCs) while using MEW and extrusion-based bioprinting B) (top view) results in hierarchical structures C) (top view), and the ability to fabricate porous constructs while including MEW D) (top view) and layered distribution in *z*-direction E) (cross section; arrow indicates where MEW mesh was positioned). eMSCs stained with DiI (red), DiO (blue/yellow), and DiD (green). Scale bars = 400 µm.
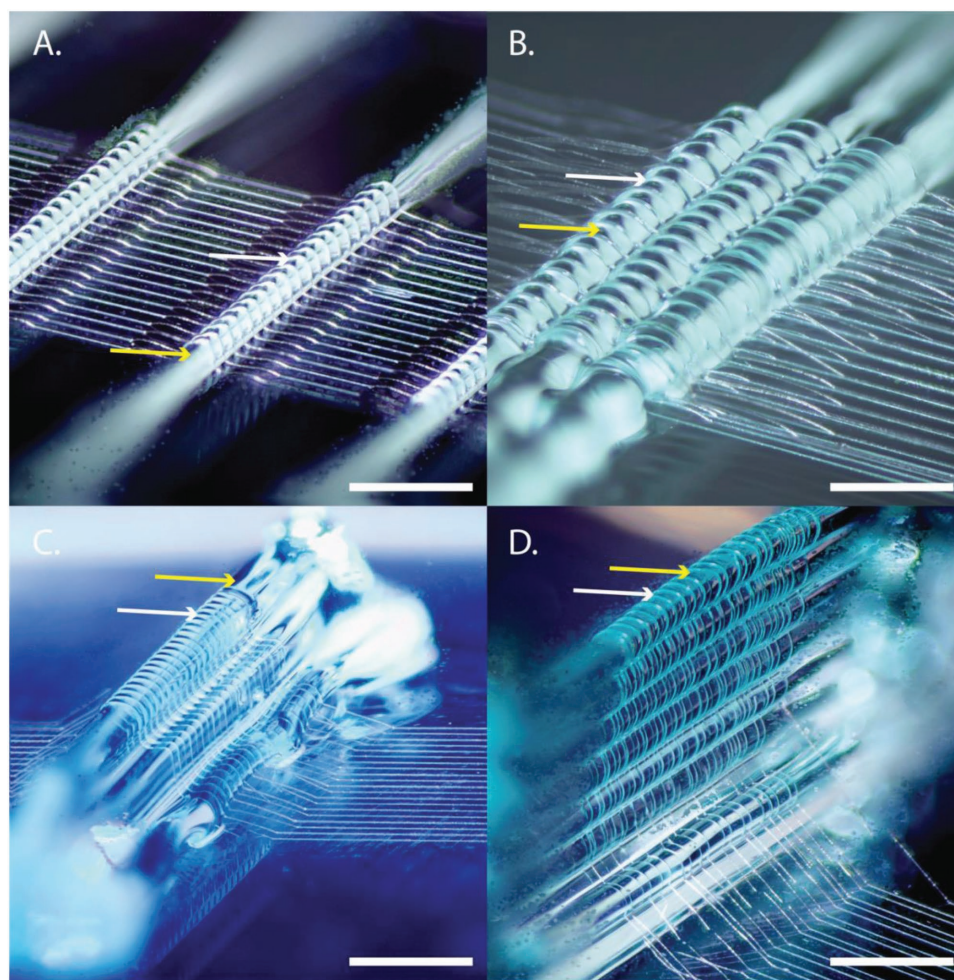
Figure 2. Toward more complex tissue architectures: using hydrogel (Pluronics, 40% w/v) to guide the direction of MEW (PCL) fibers. MEW fibers are guided over a single strand of hydrogel A), interlocked with hydrogel B). This enables more complex fiber architectures C) and out-of-plane fiber deposition D). Yellow arrows depict the hydrogel whereas the white arrows depict the PCL fiber. Scale bar = 500 µm.

(Figure 1D), which is essential when considering oxygen and nutrient supply in larger tissue constructs.[32,33] To our knowledge, we are the first to demonstrate this more refined level of controlled 3D spatial organization when combining both micrometer-scale fibers and cell-laden hydrogels.

Improvements in organization of tissue architecture are an important step toward recapitulating the complex architecture of tissues. Clearly, fibers in native tissue possess specific alignment that goes beyond the square, rectangular, or triangular structures that are typically fabricated with MEW.[34,35] We demonstrated that during the converged printing of MEW and extrusion-based hydrogel printing, the hydrogel (here 40% w/v Pluronics F127) guides the spatial 3D architecture of the PCL fibers, and that this can be in the form of a single hydrogel strand (**Figure 2**A), interlocking the hydrogel (Figure 2B), or more complex shapes such as prisms (Figure 2C). The guiding of the MEW fiber by the hydrogel can even result in MEW fibers that have an out-of-plane character (Figure 2D). Although precise control over the spatial formation of fibrous structures remains challenging, the converged printing approach improves this control over fiber deposition, which is imperative

in order to more closely mimic the fibrous component of the extracellular matrix architecture of the native tissue.

In addition to structural organization, the generation of mechanically competent constructs is crucial for the clinical application of the bioprinted constructs. We investigated the mechanical behavior of composite constructs fabricated with the proposed single-step converged printing method, compared with similar constructs obtained by the two-step cast method. Both peak and equilibrium moduli under uniaxial compression loading conditions were assessed (**Figure 3**A). The compressive peak modulus of converged printed constructs increased from 19.85 ± 7.51 kPa for gel alone to 246.84 ± 66.42 kPa for fiber-reinforced gel, whereas the compressive peak modulus of the cast constructs increased from 49.48 ± 7.81 kPa for gel alone to 278.13 ± 56.72 kPa for fiber-reinforced gel. This increase in compressive peak modulus for the cast samples is comparable to previous studies where a volume fraction of 6% was used with the same materials (PCL and 10% gelMA).[24] Additionally, the reinforcement effect remains at equilibrium where the compressive equilibrium modulus of samples increased from 11.90 ± 4.09 (printing, gel alone) to 53.02 ± 8.73 kPa (converged

1800418 (3 of 7)
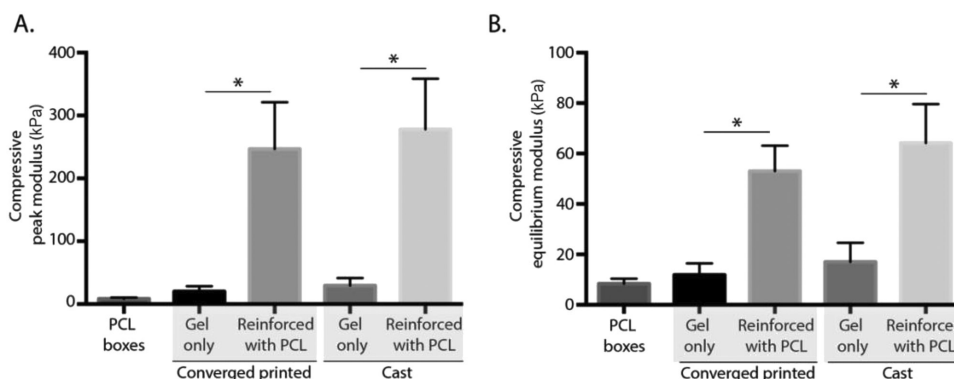
Figure 3. Convergence in a single-step approach does not affect the reinforcing effect of the MEW fibers. An increase in the compressive peak A) and equilibrium B) modulus was found when combining MEW (PCL) printing and extrusion-based hydrogel printing (10% gelMA). No differences were found between the converged printed and the cast samples. * = *p* < 0.05.

printing, reinforced gel), and from 17.02 ± 6.79 (cast, gel alone) to 64.17 ± 13.41 kPa (cast, reinforced gel) (Figure 3B). The compressive moduli of the converged printed samples did not significantly differ from the cast samples, meaning that the reinforcing effect is not affected by the converged printing approach. However, it is essential to establish a scaffold design that decreases the amount of gel between the stacking of the MEW fibers to ensure fusion of the MEW fibers in the *z*-direction, since this fusion is essential for the mechanical stability of the hydrogel–thermoplastic composites.[18] Since both the equilibrium as peak moduli of the converged printed scaffolds increased compared with printed gel only scaffolds, and no differences were found compared with the cast samples, the converged printing approach is able to increase the mechanical stability of the gelMA–PCL composites.
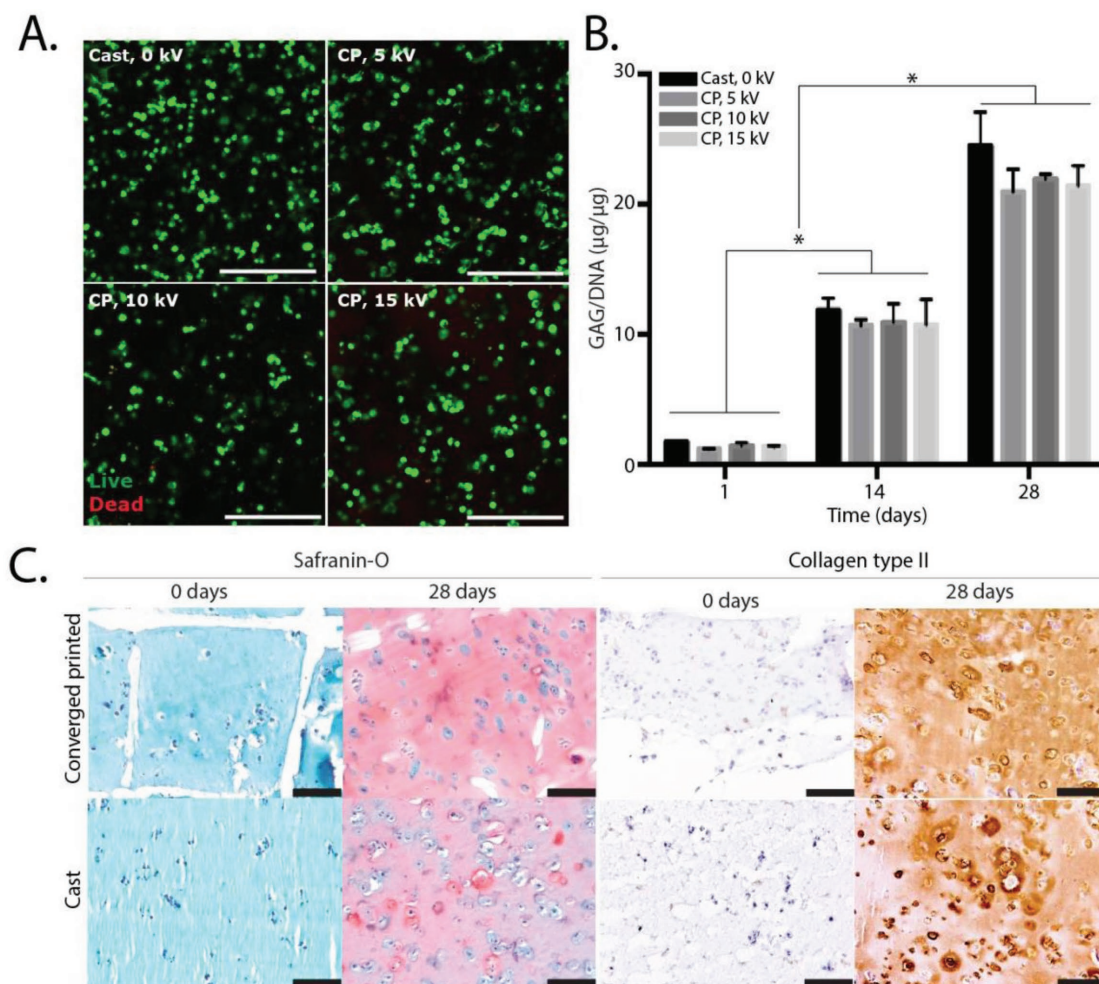
Combining MEW and hydrogel printing introduces parameters that are potentially harmful for cells embedded on extruded hydrogel structures. Thus, we demonstrated that the converged fabrication process does not affect cell survival or differentiation. First, since fiber diameters in sub-micrometer scale need to be generated, fabrication time, defined as the time needed to print the construct prior to crosslinking, is considerably higher compared with hydrogel extrusion-based bioprinting approaches. Construct fabrication time is based on a collector velocity of 80 mm s⁻¹, a fiber diameter of 13 µm, the line

spacing between the MEW fibers, and the required scaffold volume (**Figure 4**A). Second, due to the increase of fabrication time, we assessed the effect of exposure time to environmental conditions during converged printing on the metabolic activity of the embedded cells (Figure 4B). For this, eMSCs (20 × 10⁶ mL⁻¹) were encapsulated in 10% gelMA and exposed to fabrication conditions by placement into an active fabrication chamber for 0–60 min; constructs were subsequently cultured in chondrogenic differentiation medium for four weeks. Metabolic activity, compared with cast constructs not subjected to the fabrication conditions, was found to be decreased by 12%, 33%, 63%, and 80% after 15, 30, 45, and 60 min, respectively. Third, the high voltage (typically 5–15 kV) required for MEW to acquire the jet may impact cell survival.

To assess the effect of the high voltage on cell behavior, eMSCs were embedded in 10% gelMA and constantly subjected to 0, 5, 10, or 15 kV. After 14 d, eMSC viability was 92% ± 3%, 93% ± 3% 91% ± 2%, and 90% ± 2% for 0, 5, 10, and 15 kV, respectively (**Figure 5**A and Figure S1A in the Supporting Information). Furthermore, metabolic activity of the constructs that were subjected to such voltage did not decrease, compared with the control samples that were not subjected to a voltage difference (Figure S1B in the Supporting Information). In addition, as MSCs have the ability to differentiate toward multiple lineages, including bone, fat, tendon, myoblasts, neural-like
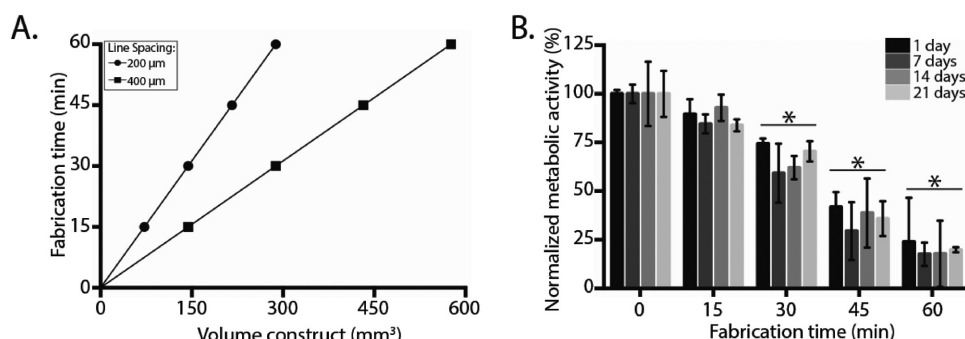
Figure 4. Effect of environmental conditions on cells. Converged printing increases printing time of constructs, which is related to the volume and line spacing of the prints A). Converged printed constructs with a volume of 100 mm³ and a line spacing of 400 µm, resulted in 10 min of printing time per construct. Incubating the hydrogel after crosslinking decreased metabolic activity of the cells B). Metabolic activity was normalized against cast control sample without incubation time. * = significant difference from an incubation time of 0 min, *p* < 0.05.

**ADVANCED
SCIENCE NEWS**
www.advancedsciencenews.com

**ADVANCED
HEALTHCARE
MATERIALS**
www.advhealthmat.de

Figure 5. MSC behavior after converged printing process. Cell viability (t = 14 d) in converged printing (CP) approach was comparable to cast control sample for all voltages used A). Chondrogenic differentiation was not compromised by the converged printing (CP) approach, showing no statistical differences in GAG/DNA compared with cast samples, for 5, 10, and 15 kV B). Safranin-O and collagen type II staining shows good proteoglycan and collagen type II distribution throughout the entire construct C). Scale bar = 100 µm, * = $p < 0.05$.

cells, and cartilage tissue, this converged printing method has potential application in multiple tissue types.[37–39] As a proof of concept that the converged printing process was not harmful for eMSCs, we specifically demonstrated the potential to form cartilage-like tissue. We first measured glycosaminoglycan's (GAGs), one of the main extracellular matrix components of cartilage, with a GAG/DNA assay over 28 d of culture. All samples showed an increase in GAG/DNA to an average of 11 ± 1 µg/µg and 22 ± 2 µg/µg after 14 and 28 d of culture, respectively. This finding was irrespective of the application of high voltage applied (Figure 5B). We confirmed this observation by safranin-O staining, which revealed that GAGs are evenly distributed throughout the samples (Figure 5C). For collagen type II, another main component of the extracellular matrix of cartilage, production was found to be increased over time in all samples, irrespective of the voltage applied (Figure 5C). No significant differences were observed for cell viability, metabolic activity, or cartilage-like matrix production between the cast and converged printed scaffolds. Hence, converged printing did not affect cell (MSC) behavior in terms of viability, metabolic

activity, and chondrogenic differentiation, and is therefore a promising biofabrication technique to fabricate hierarchical multimaterial, or multicellular structures with the potential to differentiate toward a mature tissue structure.

To our knowledge, this study demonstrates, for the first time, the successful convergence of MEW and extrusion-based hydrogel printing into a single-step manufacturing approach, improving our control over structure design and fiber writing. Our biofabrication technique allows us to grow living cells in a microenvironment with precisely controlled 3D spatial organization that more faithfully recapitulates the complex architecture of native tissues. This greatly increases the ability to fabricate clinically relevant constructs without compromising mechanical integrity, cell viability, or (chrondrogenic) differentiation.

Experimental Section

Materials: The bioink for the cell experiments was 10% (w/v) gelatin methacryloyl (gelMA) (80% DoF, synthesized as previously described[40]) because of its high chondrogenic differentiation capacity,[41] and

ADVANCED
SCIENCE NEWS
www.advancedsciencenews.com

ADVANCED
HEALTHCARE
MATERIALS
www.advhealthmat.de

the crosslinker Irgacure 2959 (BASF, Ludwigshafen, Germany) was dissolved in phosphate-buffered saline (PBS) at 0.1% w/v. Pluronics F127 hydrogel (40% w/v in PBS) was used as a model-ink to study the ability to guide MEW fibers with a hydrogel template because of its high shape fidelity. Medical-grade polycaprolactone (PCL) (PURASORB PC 12, Lot# 1412000249, 03/2015, Corbion Inc., Gorinchem, The Netherlands) was used as MEW material.

Cells: Equine-derived mesenchymal stromal cells (eMSCs) were harvested at passage 3, embedded in 10% (w/v) gelMA at 20×10^6 cells mL^{-1}, and subsequently cultured in chondrogenic differentiation medium consisting of DMEM 41965 (Gibco) supplemented with penicillin/streptomycin (1%, Gibco), L-ascorbic acid-2-phosphate (0.2×10^{-3} M, Sigma Aldrich), ITS + Premix Universal Culture Supplement (1%, Corning), dexamethasone (0.1×10^{-6} M, Sigma Aldrich) and recombinant human TGF-ß1 (10 ng mL^{-1}) for 28 d, medium was refreshed twice per week. To show control over cell deposition, eMSCs were labeled with a Vybrant cell labeling kit (Thermo Fischer Scientific), according to manufacturer's protocol prior to encapsulation in gelMA. Confocal imaging was used to analyze cell distribution (Leica SP8X). To assess the effect of the fabrication conditions on the constructs, eMSC-laden 10% gelMA disks were cast, crosslinked for 15 min (UVP CL-1000 Ultraviolet Crosslinker), incubated for 0, 15, 30, 45, or 60 min, and cultured for 28 d. Metabolic activity was measured with an Alamar Blue staining (Resazurin sodium salt, Alfa Aesar) and cartilage-like matrix formation was quantified with a GAG/DNA analysis [Dimethylmethylene blue (DMMB, Sigma Aldrich, Picogreen, Quant-iT, Thermo Fischer Scientific)]. To evaluate if the cells were affected by the converged printing process, alternating layers of PCL fibers and gelMA (10% w/v; encapsulated with eMSCs) were fabricated. PCL fibers were deposited at 85 °C, with a collector velocity of 80 mm s^{-1}, pressure of 1.0 bar, collector distance of 6.0 mm, and with a voltage of 5, 10, or 15 kV. After printing, all samples were cultured for 28 d in chondrogenic differentiation medium and analyzed for viability, metabolic activity, and chondrogenic differentiation with a LIVE/DEAD assay (Calcein, Ethidium homodimer, Thermo Fischer Scientific), GAG/DNA, Safranin-O, and collagen type II staining, respectively. An eMSC-laden cast disk was used as a control.

Scaffold Fabrication - Cast Scaffolds: Ten percent (cell-laden) gelMA samples were cast in disks using a Teflon mold at 15 –18 °C and UV crosslinked for 15 min (UVP CL-1000 Ultraviolet Crosslinker).

Scaffold Fabrication - Converged Printed Scaffolds: Converged printing was performed in a single-step approach (3DDiscovery Evolution, regenHU). Scaffold design was either layer-by-layer deposition of MEW fibers and extrusion-based bioprinted (cell-laden) hydrogel, or deposition of gel inside the MEW squared structures (boxes). PCL fibers were deposited at 85 °C, with a collector velocity of 80 mm s^{-1}, 5.0 kV, 1.0 bar, and at a collector distance of 6.0 mm. Ten percent w/v gelMA was extruded with a pressure of 0.5 bar, at 15–18 °C, and a collector velocity of 25 mm s^{-1}. To investigate the possibilities of using a hydrogel to guide 3D MEW fiber deposition, different layers of hydrogel (Pluronics, 40% w/v, extruded with a pressure of 1.0 bar and a collector velocity of 22 mm s^{-1}, at room temperature) were printed in the *x*-axis direction, after which the MEW fiber was deposited in *y*-axis direction.

Mechanical Analysis: To analyze the mechanical properties of converged printed scaffolds, alternating layers of MEW PCL and 10% gelMA without cells were deposited. The MEW boxes had a line spacing of 400 μm and total scaffold height was 1.8 mm. The elastic peak and equilibrium moduli were assessed by unconfined compression using dynamical mechanical analysis (Q800, TA Instruments). Samples were prestrained at 20% strain followed by isostrain of 15 min. As a control, cast 10% gelMA disks (height = 2 mm, diameter = 6 mm) with and without MEW reinforcement were analyzed.

Statistics: For samples that were used for mechanical analysis, an *n* = 5 was applicable; for samples including cells, an *n* = 3 was used. For the quantitative data, a one-way ANOVA, post hoc Bonferroni was performed to test differences between groups. Differences were found to be significant when $p < 0.05$.

Supporting Information

Supporting Information is available from the Wiley Online Library or from the author.

Acknowledgements

Conflict of Interest

The authors declare no conflict of interest.

Keywords

[1] J. Groll, T. Boland, T. Blunk, J. A. Burdick, D. W. Cho, P. D. Dalton, B. Derby, G. Forgacs, Q. Li, V. A. Mironov, L. Moroni, M. Nakamura, W. M. Shu, S. Takeuchi, G. Vozzi, T. B. F. Woodfield, T. Xu, J. J. Yoo, J. Malda, *Biofabrication* **2016**, *8*, 013001.

[2] F. P. W. Melchels, M. A. N. Domingos, T. J. Klein, J. Malda, P. J. Bartolo, D. W. Hutmacher, *Prog. Polym. Sci.* **2012**, *37*, 1079.

[3] R. Chang, Y. Nam, W. Sun, *Tissue Eng., Part C* **2008**, *14*, 157.

[4] D. W. Hutmacher, *Nat. Mater.* **2010**, *9*, 90.

[5] B. Derby, *Science* **2012**, *338*, 921.

[6] T. J. Klein, J. Malda, R. L. Sah, D. W. Hutmacher, *Tissue Eng., Part B* **2009**, *15*, 143.

[7] A. P. Hollander, S. C. Dickinson, W. Kafienah, *Stem Cells* **2010**, *28*, 1992.

[8] R. Levato, W. R. Webb, I. A. Otto, A. Mensinga, Y. D. Zhang, M. van Rijen, R. van Weeren, I. M. Khan, J. Malda, *Acta Biomater.* **2017**, *61*, 41.

[9] X. Ren, F. Y. Wang, C. Chen, X. Y. Gong, L. Yin, L. Yang, *BMC. Musculoskeletal. Disorders* **2016**, *17*, 301.

[10] D. B. Kolesky, R. L. Truby, A. S. Gladman, T. A. Busbee, K. A. Homan, J. A. Lewis, *Adv. Mater.* **2014**, *26*, 3124.

[11] B. Byambaa, N. Annabi, K. Yue, G. Trujillo-de Santiago, M. M. Alvarez, W. Jia, M. Kazemzadeh-Narbat, S. R. Shin, A. Tamayol, A. Khademhosseini, *Adv. Healthcare Mater.* **2017**, *6*, 1700015.

[12] L. Horvath, Y. Umehara, C. Jud, F. Blank, A. Petri-Fink, B. Rothen-Rutishauser, *Sci. Rep.* **2015**, *5*, 7974.

[13] J. Malda, J. Visser, F. P. Melchels, T. Jungst, W. E. Hennink, W. J. A. Dhert, J. Groll, D. W. Hutmacher, *Adv. Mater.* **2013**, *25*, 5011.

[14] F. T. Moutos, L. E. Freed, F. Guilak, *Nat. Mater.* **2007**, *6*, 162.

[15] I. C. Liao, F. T. Moutos, B. T. Estes, X. Zhao, F. Guilak, *Adv. Funct. Mater.* **2013**, *23*, 5833.

[16] M. Akbari, A. Tamayol, V. Laforte, N. Annabi, A. H. Najafabadi, A. Khademhosseini, D. Juncker, *Adv. Funct. Mater.* **2014**, *24*, 4060.

[17] H. W. Kang, S. J. Lee, I. K. Ko, C. Kengla, J. J. Yoo, A. Atala, *Nat. Biotechnol.* **2016**, *34*, 312.

[18] V. H. M. Mouser, A. Abbadessa, R. Levato, W. E. Hennink, T. Vermonden, D. Gawlitta, J. Malda, *Biofabrication* **2017**, *9*, 015026.

[19] W. Schuurman, V. Khristov, M. W. Pot, P. R. van Weeren, W. J. A. Dhert, J. Malda, *Biofabrication* **2011**, *3*, 021001.

[20] J. S. Lee, J. M. Hong, J. W. Jung, J. H. Shim, J. H. Oh, D. W. Cho, *Biofabrication* **2014**, *6*, 024103.

[21] K. W. M. Boere, M. M. Blokzijl, J. Visser, J. E. A. Linssen, J. Malda, W. E. Hennink, T. Vermonden, *J. Mater. Chem. B* **2015**, *3*, 9067.

[22] D. W. Hutmacher, T. Schantz, I. Zein, K. W. Ng, S. H. Teoh, K. C. Tan, *J. Biomed. Mater. Res.* **2001**, *55*, 203.

[23] M. Darnell, D. J. Mooney, *Nat. Mater.* **2017**, *16*, 1178.

[24] J. Visser, F. P. Melchels, J. E. Jeon, E. M. van Bussel, L. S. Kimpton, H. M. Byrne, W. J. Dhert, P. D. Dalton, D. W. Hutmacher, J. Malda, *Nat. Commun.* **2015**, *6*, 6933.

[25] G. Hochleitner, T. Jungst, T. D. Brown, K. Hahn, C. Moseke, F. Jakob, P. D. Dalton, J. Groll, *Biofabrication* **2015**, *7*, 035002.

[26] T. D. Brown, P. D. Dalton, D. W. Hutmacher, *Adv. Mater.* **2011**, *23*, 5651.

[27] P. D. Dalton, T. D. Brown, D. W. Hutmacher, *J. Tissue Eng. Regener. Med.* **2012**, *6*, 372.

[28] M. de Ruijter, A. Hrynevich, J. N. Haigh, G. Hochleitner, M. Castilho, J. Groll, J. Malda, P. D. Dalton, *Small* **2017**, *14*, 1702773.

[29] M. Castilho, D. Feyen, M. Flandes-Iparraguirre, G. Hochleitner, J. Groll, P. A. F. Doevendans, T. Vermonden, K. Ito, J. P. G. Sluijter, J. Malda, *Adv. Healthcare Mater.* **2017**, *6*, 1700311.

[30] G. Criscenti, A. Vasilevich, A. Longoni, C. De Maria, C. A. van Blitterswijk, R. Truckenmuller, G. Vozzi, J. De Boer, L. Moroni, *Acta Biomater.* **2017**, *55*, 310.

[31] W. Liu, M. A. Heinrich, Y. Zhou, A. Akpek, N. Hu, X. Liu, X. Guan, Z. Zhong, X. Jin, A. Khademhosseini, Y. S. Zhang, *Adv. Healthcare Mater.* **2017**, *6*, 1601451.

[32] J. Zeltinger, J. K. Sherwood, D. A. Graham, R. Mueller, L. G. Griffith, *Tissue Eng.* **2001**, *7*, 557.

[33] J. Malda, J. Rouwkema, D. E. Martens, E. P. le Comte, F. K. Kooy, J. Tramper, C. A. van Blitterswijk, J. Riesle, *Biotechnol. Bioeng.* **2004**, *86*, 9.

[34] O. Bas, E. M. De-Juan-Pardo, C. Meinert, D. D'Angella, J. G. Baldwin, L. J. Bray, R. M. Wellard, S. Kollmannsberger, E. Rank, C. Werner, T. J. Klein, I. Catelas, D. W. Hutmacher, *Biofabrication* **2017**, *9*, 025014.

[35] T. D. Brown, P. D. Daltona, D. W. Hutmacher, *Prog. Polym. Sci.* **2016**, *56*, 116.

[36] J. N. Haigh, Y. M. Chuang, B. Farrugia, R. Hoogenboom, P. D. Dalton, T. R. Dargaville, *Macromol. Rapid Commun.* **2015**, *37*, 93.

[37] D. J. Prockop, *Science* **1997**, *276*, 71.

[38] A. J. Friedenstein, U. F. Gorskaja, N. N. Kulagina, *Exp. Hematol.* **1976**, *4*, 267.

[39] S. Wakitani, T. Saito, A. I. Caplan, *Muscle Nerve* **1995**, *18*, 1417.

[40] F. P. W. Melchels, W. J. A. Dhert, D. W. Hutmacher, J. Malda, *J. Mater. Chem. B* **2014**, *2*, 2282.

[41] B. J. Klotz, D. Gawlitta, A. J. W. P. Rosenberg, J. Malda, F. P. W. Melchels, *Trends Biotechnol.* **2016**, *34*, 394.